

Geostatistical Analysis for Landslide Susceptibility Mapping in Coonoor and Kothagiri Taluks, Nilgiri District, Tamil Nadu

Uvaraj S.^{1*} and Neelakantan R.²

1. Department of Remote Sensing, Bharathidasan University, Tiruchirappalli, Tamil Nadu, INDIA

2. Department of Industries and Earth Sciences, Tamil University, Thanjavur, Tamil Nadu, INDIA

*uvaraj.s@bdu.ac.in

Abstract

In the mountainous regions, landslides are common to cause enormous losses of life and properties. During the monsoon period, frequent landslides are occurring in Coonoor and Kothagiri taluks. The present study is to produce the landslide susceptibility mapping with the help of GIS technology using geostatistical analysis. To determine the relative effect (RE) model, the landslide causative factors were analyzed by calculating the ratio of the unit area per each class and area of previous landslide locations. The landslide inventory map was prepared using data from the state highways department and an extensive field survey. In total, 118 landslide locations were identified and mapped in GIS; out of that, 83 (70 %) locations were selected for training and the remaining 35 (30 %) cases were used for the model validation. The relative effect model, landslide susceptibility map classified the area into three zones like high, moderate and low. The final map was validated using Relative landslide density index (R-index) method. The validation of the results showed that the values of 263.73 in the high susceptible zone were indicating that R-index increases with the level of susceptibility. Thus, it was considered that the RE models confer acceptable and reliable results. Based on these results, it is concluded that the landslide susceptibility map can be used to reduce damage associated with landslides, land use planning and various developmental activities on the area.

Keywords: Landslide susceptibility, Coonoor and Kothagiri, Relative effect model, GIS, R-index.

Introduction

Landslides are one of the important disasters in mountainous regions and every year they cause huge loss of life and property. The Nilgiri Mountain is an important tourist place in South India and attracts a large number of tourists due to climate and landscape. Due to developmental activities, the natural vegetations are degraded. The main problems in the study are the landslides and heavy soil erosion induced by torrential rain and flooding. In the Nilgiri, during the rainy periods the pore pressure increases in the soils which leads to landslide occurrences.²⁴ One of the most difficult problems concerning landslide hazards in places like Nilgiris is dealing with existing urban areas where buildings are

constructed or they are close to a landslide. The ideal approach in this situation is to abstain further development in high-risk landslide prone areas, limit existing-user rights to rebuild and limit the use of buildings. Still no clear prediction system is readily available for landslide occurrences like the size, location that would cause casualties, harm, or rupture to an existing standard of safety. In the landslide prone areas, there are no warning signs and indications of vulnerable slopes where designated. Hence, the present research problem has been chosen for analysis of landslide and its causative factors.

To generate the landslide susceptibility mapping is an important task for geoscientists, planners and local administrations, as knowledge about the socioeconomic worth of landslides has increased worldwide.⁹ Landslide susceptibility indicates to the probability of landslide occurrence in a region based on the relationship between landslide influencing factors with existing landslide locations.⁸ The type, spatial extent and intensity of past and present landslides in the study area relate to the landslide susceptibility which assesses the probable areas for future landsliding, but the frequency or timing is not incorporated.^{2,6} In recent years, various methods and techniques are used for landslide susceptibility maps by using GIS such as frequency ratio methods,^{3,5,16,23} logistic regression models,^{1,14,18,19} analytical hierarchy process methods,^{11,13,15,31} fuzzy logic methods^{22,26,28} and artificial neural network method.^{10,25,27,30} The relative effect method has also been applied to landslide susceptibility mapping.^{4,12,20,21} Van Westen et al²⁹ used a function for landslide zonation that almost corresponds with the relative effector function, but the benefit of the relative effect method is ranking of effective factors in the landslide zonation.

Several methods have been suggested and utilized for landslide susceptibility mapping. Among the various methods, a statistical model was developed with the help of GIS techniques to map landslide hazard zones in a hilly region.²¹ Landslide susceptibility and hazard maps are utilized for identifying future landslide-prone areas and also proper planning for the landscape could be designed through statistically based prediction models. With this background, the present study attempts relative effect-based geostatistical techniques applied for landslide susceptibility mapping. The purpose of this research is to define a suitable method with the ability to forecast landslide hazard through the application of a relative effect method.

Study Area

The study area Coonoor and Kothagiri revenue taluks of Nilgiri district falls in the northern and southern part of the Nilgiri hill ranges. The total coverage of the study area is 637.62km² and covered by the survey of India (SOI) topographic maps Nos. 58 A/11, 58 A/12, 58 A/14, 58 A/15, 58 E/2 and 58 E/3. The geographical location of the study area is 76°40' 26" to 77° 00' 52" E longitudes and 11° 14' 36" to 11° 34' 43" N latitudes which is shown in fig. 1. The study area is rising abruptly from the surrounding plains to an elevation of 1370m AMSL and it is bound by Ootacamund town in the northwest and northern portion in Moyar River. The entire Coonoor and Kothagiri taluks are benefitted by the rain of NE monsoon.

Preparation of Landslide Influencing Factors: To approach the relative effect model, a spatial database that considers landslide causative parameters was designed and constructed. The constructed spatial database is listed in table 1. The remote sensing technology is associated with ground check and is helping to map the spatial distributions of various causative factors. Active and passive slope, concave-plain-convex slope, drainage density, dissected and

un-dissected slope, lithology, geomorphology, lineament density, lineament frequency, lineament intersection density, land use/land cover, rainfall, regolith cover, shallow-moderate-steep slope, soil and water level are considered for landslide susceptibility mapping. In general, landslide susceptibility studies assumed that the future landslides must occur with the same causative factors of prior landslides.^{17,32} According to this assumption, one of the foremost data landslide inventory maps that are needed are significant for landslide susceptibility mapping, since they show the distribution and characteristics of the past and present landslides in their geospatial locations. Landslide inventory mapping has been carried out by a collection of existing historical reports from highways department and extensive field survey.

This inventory map has shown that about 118 landslide locations were identified and mapped in a GIS platform (fig. 2); out of that, 83 (70%) locations were randomly selected for training and the remaining 35 (30%) cases were used for the purpose of model validation. Some of the field observations of the landslide incidences are shown in fig. 3. The main types of landslides occurring in the study area are: Falling, Subsiding, Sliding and Flowing.

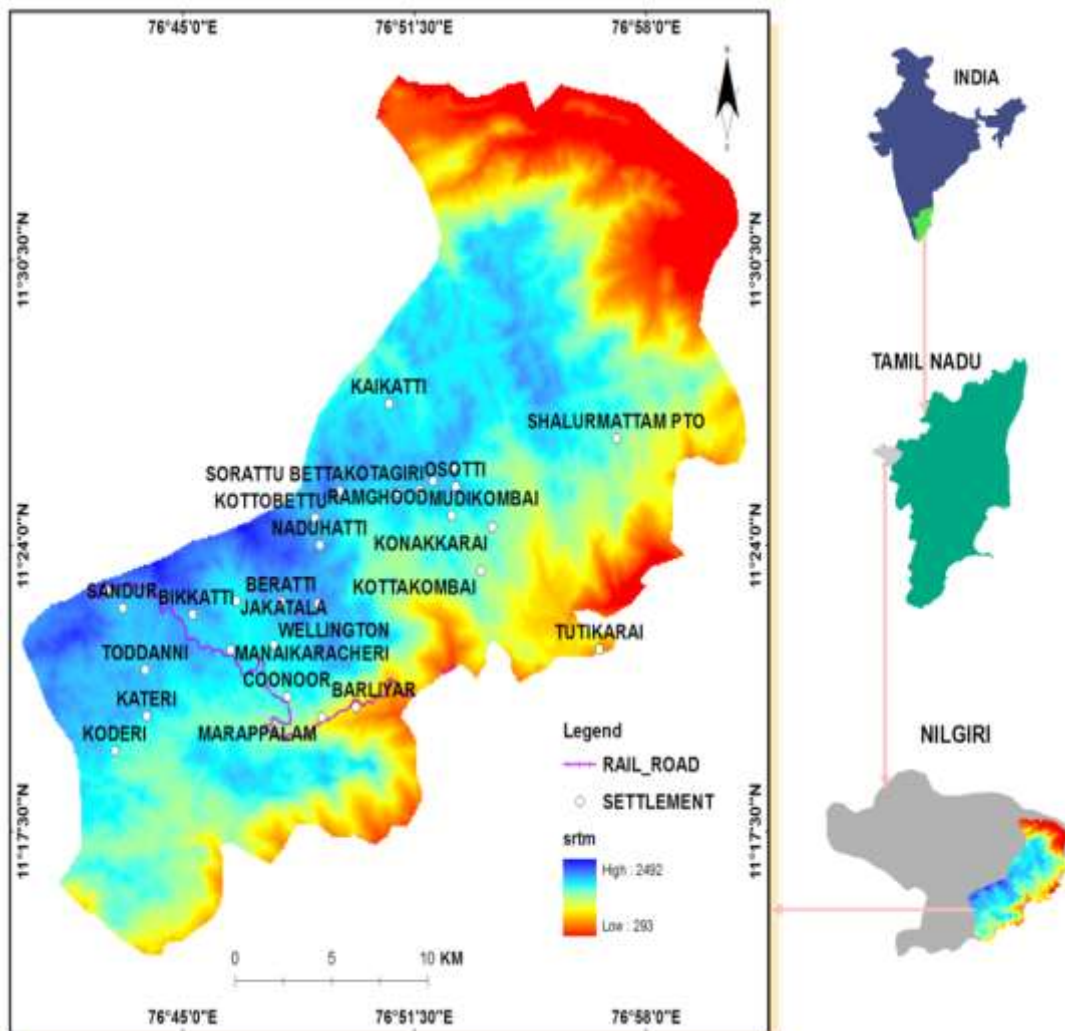


Figure 1: Location and digital elevation model (DEM) of Coonoor and Kothagiri taluks

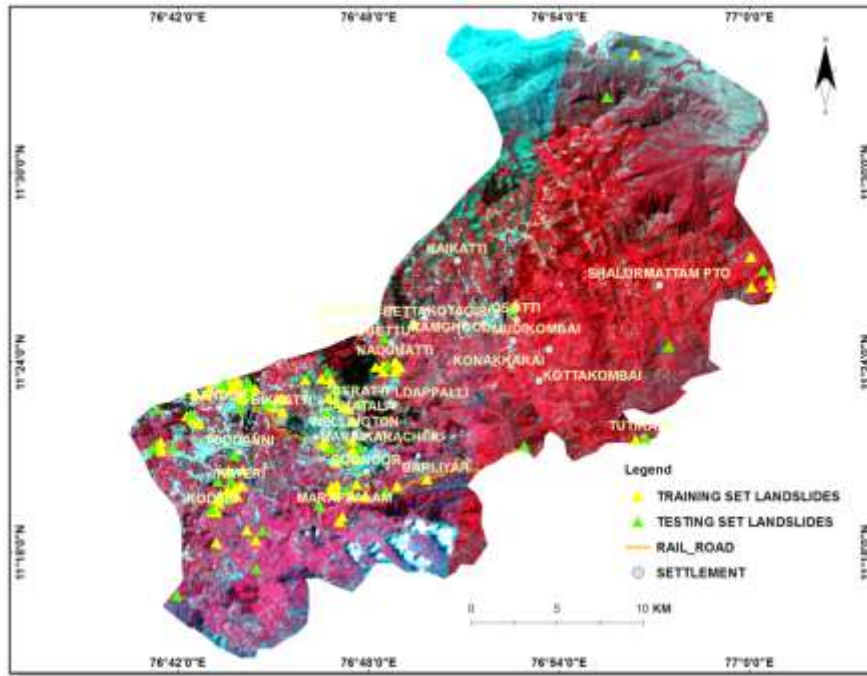


Figure 2: IRS P6 LISS IV – FCC image with landslide locations



Debris slide near Lovedale



Achanakal debris flow



Rock fall along railway line of Coonoor –
Mettupalayam road



Landslide at Ooty - Coonoor ghat road

Figure 3: Field observations of landslides

The slope is a major causative factor/parameter for the landslide occurrences. Hence, detailed geomorphic based slope classifications like active and passive slope, concave-plain-convex slope, dissected and un-dissected slope and

shallow-moderate-steep slope have been interpreted by using topographical, aerial photograph, IRS P6 LISS IV satellite data and SRTM data. Based on the vegetation cover, active and passive slopes are identified and mapped.

Active slopes were interpreted by the presence of barren rocks and low vegetation covers. The dense vegetation covers were separated by passive slopes. Concave-plain-convex slopes were demarcated by using large format aerial photographs. The convex slopes show convexity and mound shape. The slope showing a smoother and plain configuration was marked as plain slope. The slopes having boat shapes and bowl shapes which were invariably filled with vegetation were marked as plain slopes. Dissecting and undissecting slopes were classified by the presence of drainage density and gullies. The slopes with more drainage density and gullies were demarcated as dissected and less drainage density was marked as un-dissected slope. By using a 90m resolution of SRTM data, the slope classes were categorized into shallow (0-22°), moderate (22-44°) and steep (44-66°) slope. The drainage map was prepared by using SOI toposheets with 1:50,000 scale of the drainage map; density is calculated and classified into very high density, high density, moderate and low density. The lithology map is prepared from the GSI published geological map. The study area mainly consists of bulk forms of charnockites rock units.

The detailed geomorphic features were interpreted from IRS P6 satellite data and created DEM with topographical data. The interpretation of geomorphic classes such as summit and geomorphic features was identified and mapped. Highly dissected deflection slope, less dissected undulating plateau and ridge type structural hills are categorized under summit features. The fracture valley, valley fill, intermontane valley, river, tank, shallow pediment and flood plains are assorted under geomorphic features. In the study area lineaments in different directions were interpreted using the FCC satellite image; the lineament density map was prepared by superimposing a vector grid of 1000m×1000m over the lineament map. The lineament density was calculated to measure the total length of the lineament per grid and density contour was generated and classified into low density (0-1.5), moderate density (1.5-3.0), high density (3-4.5) and very high density (<4.5). The lineament frequency values of 0 to 10 were calculated by counting the number of lineaments present in each grid and classified into low frequency (0-2.5), moderate frequency (2.5-5), high frequency (5-7.5) and very high frequency (<7.5). The number of lineament intersection present in each grid was counted which will give the lineament intersection density values of 0 to 13 such as classified into low intersection density (0-3), moderate intersection density (3-6), high intersection density (6-9) and very high intersection density (<9).

The stability of the slope is disturbed by the different land use practices. The uncertain land use practices due to anthropogenic activities may lead to landslide occurrences. By using the visual interpretation of the satellite image, the various land use/land cover classes are interpreted such as barren rocky area, crop land, dense forest, fairly dense forest, forest plantation, mixed built-up land, open forest, scrub

forest and wetland. The rainfall information was collected for 35 years from the PWD groundwater and the mean annual rainfall was calculated and the contours were generated in the GIS platform. In the study area the average annual rainfall ranges between 1200-1400mm. To understand the study area degree of weathering of the rock and soil types, the drainage sections, railway cutting and road cutting were thoroughly surveyed and from the geophysical data, the thickness of topsoil and the weathered zone were also noted down (Regolith cover). These were plotted in the respective locations and contoured. The thickness of weathered zone varies from as low as 5.5m to as high as 37m in the area. The soil information has been collected from soil survey and land use board and study area soil map in GIS environment was prepared. It has been observed that most of the study area highly eroded clayey soil followed by moderately eroded gravelly soils. The gravelly clay soil is also observed in the northern part of the study area and other calcareous cracking clay soil, calcareous loamy soils. The study area water level data has been collected from Central Ground Water Board (CGWB) and the same has been converted into digital format by using GIS environment.

Methodology

In this study, geostatistical approach (i.e.) Relative Effect method was applied to generate landslide susceptibility mapping in GIS environment. In RE method, it is necessary to assess the relative effect of each parameter on the landslide occurrence by calculating relative landslide density in each parameter. The relative effect of each class of parameters was also determined by dividing the landslide area per each class to the area of each class. The function that is used in this method is logarithmic. The training sets landslide locations 83 (70 %) were crossed to the landslide triggering parameters such as active and passive slope, concave-plain-convex slope, shallow-moderate-steep slope, dissected and un-dissected slope, lithology, drainage density, geomorphology, lineament density, lineament frequency, lineament intersection density, land use/land cover, rainfall, regolith cover, soil and water level. The relative values of each class (C) on occurred landslides were calculated through dividing the each class area (a) to total area (A) and were applied to the parameters respectively.

$$C = \frac{a}{A} \times 100 \quad (1)$$

A landslide percentage of the each unit (S) was calculated using a dividing landslide area in each unit (*sld*) to a total landslide area in the study area:

$$S = \frac{sld}{SLD} \times 100 \quad (2)$$

Consequently, the relative effect of each parameter (RE) was calculated based on the logarithm of landslide percentage of each unit (S) to the coverage percent of each parameter (C) plus epsilon to prevent of zero making:

$$RE = \log\left(\frac{S}{C}\right) + \epsilon \tag{3}$$

In the relationship analysis, there are three cases of estimating a relative effect of each unit depending on its RE.

- RE is greater than zero means that it has an effect of increasing landslide risk (*Positive Effect*).
- RE is less than zero means that it has an effect of decreasing landslide risk (*Negative Effect*).
- RE is zero means that it has no effect of decreasing or increasing landslide risk (*Zero Effect*).

The results of cross function containing the rate of occurred landslides in the classes of each parameter are shown in table 1.

Landslide Susceptibility Mapping: The calculated RE values were added to the attribute table of each parameter, these thematic layers were converted into a raster layer based on the relative effect field values. All the raster layers were integrated in the GIS environment by using raster calculator option in spatial analyst tool. Then, the landslide susceptibility index of the study area was computed by sum relative effect of parameters on the unit area.

$$LSI = \sum(RE_{active-passive\ slope} + RE_{concave-plain-convex\ slope} + RE_{drainage\ density} \dots) \tag{4}$$

where RE is the rating of each factor’s type or range.

The relative effect of the individual layers and LSI was calculated based on the minimum and maximum values; the landslide susceptibility map has been prepared and relative effect model was developed as shown in fig. 4. The LSI has a minimum value of (-5.340) and a maximum value of (4.389) with a mean value of (-1.369) and a standard deviation of 2.189. The range of minimum and maximum values was equally divided into three categories and classified as high (1.146-4.389), moderate (-2.096-1.146) and low (-5.340--2.096) susceptible zones.

The relative effect model shows that the area has been divided into three hazard classes. In the hazard classes, 19.49% of the area comes under the high, 30.99% of the area in moderate and 49.52% of the area comes in low hazard categories (Table 2). In area wise graphical representation of a landslide susceptible zone was also prepared as shown in fig. 5.

Table 1
Relative effect values for landslide causative parameters

| Domain Factors | Class | % Coverage | % Slide | Relative Effect (RE) |
|------------------------------|--|------------|---------|----------------------|
| Active – Passive Slope | Active | 42.88 | 44.58 | 0.02 |
| | Passive | 57.12 | 55.42 | -0.01 |
| Concave–Plain–Convex Slope | Concave | 4.78 | 8.43 | 0.25 |
| | Plain | 7.41 | 4.82 | -0.19 |
| | Convex | 87.81 | 86.75 | -0.01 |
| Drainage Density | Very high | 8.35 | 0.00 | 0.00 |
| | High | 27.36 | 27.71 | 0.01 |
| | Moderate | 41.39 | 48.19 | 0.07 |
| | Low | 22.90 | 24.10 | 0.02 |
| Dissected–Un dissected Slope | Dissected | 12.58 | 31.33 | 0.40 |
| | Un dissected | 87.42 | 68.67 | -0.10 |
| Lithology | Charnockite | 96.22 | 96.39 | 0.00 |
| | Garnetiferous quartzo feldspathic gneiss | 1.50 | 3.61 | 0.38 |
| | Fissile hornblende-biotite gneiss | 1.26 | 0.00 | 0.00 |
| | Granitoid gneiss | 0.61 | 0.00 | 0.00 |
| | Ultramafic | 0.42 | 0.00 | 0.00 |
| Geomorphology | River | 0.16 | 0.00 | 0.00 |
| | Tank | 0.05 | 0.00 | 0.00 |
| | Flood plain | 0.94 | 0.00 | 0.00 |
| | Valley fill | 1.90 | 0.00 | 0.00 |
| | Fracture valley | 0.99 | 1.20 | 0.09 |
| | Intermontane valley | 0.79 | 0.00 | 0.00 |
| | Less dissected undulating plateau | 28.46 | 45.78 | 0.21 |
| | Moderately dissected plateau | 27.80 | 15.66 | -0.25 |
| | Highly dissected deflection slope | 28.63 | 32.53 | 0.06 |

| | | | | |
|--------------------------------|--------------------------------------|-------|-------|-------|
| | Structural hill | 3.05 | 3.61 | 0.07 |
| | Shallow pediment | 2.82 | 0.00 | 0.00 |
| | Ridge type structural hill | 4.41 | 1.20 | -0.56 |
| Lineament Density | | | | |
| | Very high (<4.5) | 6.11 | 16.87 | 0.44 |
| | High (3-4.5) | 16.29 | 38.55 | 0.37 |
| | Moderate (1.5-3.0) | 34.05 | 34.94 | 0.01 |
| | Low (0-1.5) | 43.55 | 9.64 | -0.66 |
| Lineament Frequency | | | | |
| | Very high (<7.5) | 6.09 | 8.43 | 0.14 |
| | High (5-7.5) | 16.67 | 45.78 | 0.44 |
| | Moderate (2.5-5) | 31.42 | 32.53 | 0.02 |
| | Low (0-2.5) | 45.82 | 13.25 | -0.54 |
| Lineament Intersection Density | | | | |
| | Very high (<9) | 1.19 | 1.20 | 0.00 |
| | High (6-9) | 7.43 | 20.48 | 0.44 |
| | Moderate (3-6) | 23.41 | 43.37 | 0.27 |
| | Low (0-3) | 67.97 | 34.94 | -0.29 |
| Land use/Land Cover | | | | |
| | Mixed Built-up land | 5.71 | 28.92 | 0.70 |
| | River | 0.19 | 0.00 | 0.00 |
| | Tank | 0.04 | 0.00 | 0.00 |
| | Forest plantation | 27.37 | 31.33 | 0.06 |
| | Dense forest | 31.47 | 19.28 | -0.21 |
| | Fairly dense forest | 7.09 | 10.84 | 0.18 |
| | Open forest | 13.88 | 6.02 | -0.36 |
| | Scrub forest | 11.62 | 3.61 | -0.51 |
| | Barren rocky | 0.93 | 0.00 | 0.00 |
| | Wet land | 0.15 | 0.00 | 0.00 |
| | Crop land | 1.55 | 0.00 | 0.00 |
| Rainfall | | | | |
| | 418.39 – 824.67 | 2.43 | 1.20 | -0.30 |
| | 824.67 – 1230.95 | 5.67 | 7.23 | 0.11 |
| | 1230.95 – 1637.23 | 59.99 | 14.46 | -0.62 |
| | 1637.23 – 2043.51 | 31.91 | 77.11 | 0.38 |
| Regolith Cover | | | | |
| | 5.5 – 10.8 | 3.85 | 14.46 | 0.57 |
| | 10.8 – 16 | 90.85 | 63.86 | -0.15 |
| | 16 – 21.2 | 4.14 | 13.25 | 0.50 |
| | 21.2 – 26.5 | 0.56 | 4.82 | 0.93 |
| | 26.5 – 31.7 | 0.37 | 0.00 | 0.00 |
| | 31.7 - 37 | 0.22 | 3.61 | 1.22 |
| Shallow–Moderate–Steep Slope | | | | |
| | Shallow (0-22°) | 38.70 | 26.51 | -0.16 |
| | Moderate (22-44°) | 41.25 | 65.06 | 0.20 |
| | Steep (44-66°) | 20.05 | 8.43 | -0.38 |
| Soil | | | | |
| | Moderately eroded gravelly soil | 2.66 | 16.87 | 0.80 |
| | Highly eroded clayey soil | 79.68 | 81.93 | 0.01 |
| | Calcareous loamy soil | 2.58 | 0.00 | 0.00 |
| | Gravelly clay soil | 0.75 | 0.00 | 0.00 |
| | Gravelly loamy soil with escarpments | 8.98 | 1.20 | -0.87 |
| | Calcareous cracking clay soil | 5.36 | 0.00 | 0.00 |
| Water Level | | | | |
| | 1.36 – 1.87 | 33.80 | 84.34 | 0.40 |
| | 1.87 – 2.39 | 42.74 | 13.25 | -0.51 |
| | 2.39 – 2.91 | 19.60 | 1.20 | -1.21 |
| | 2.91 – 3.43 | 3.87 | 1.20 | -0.51 |

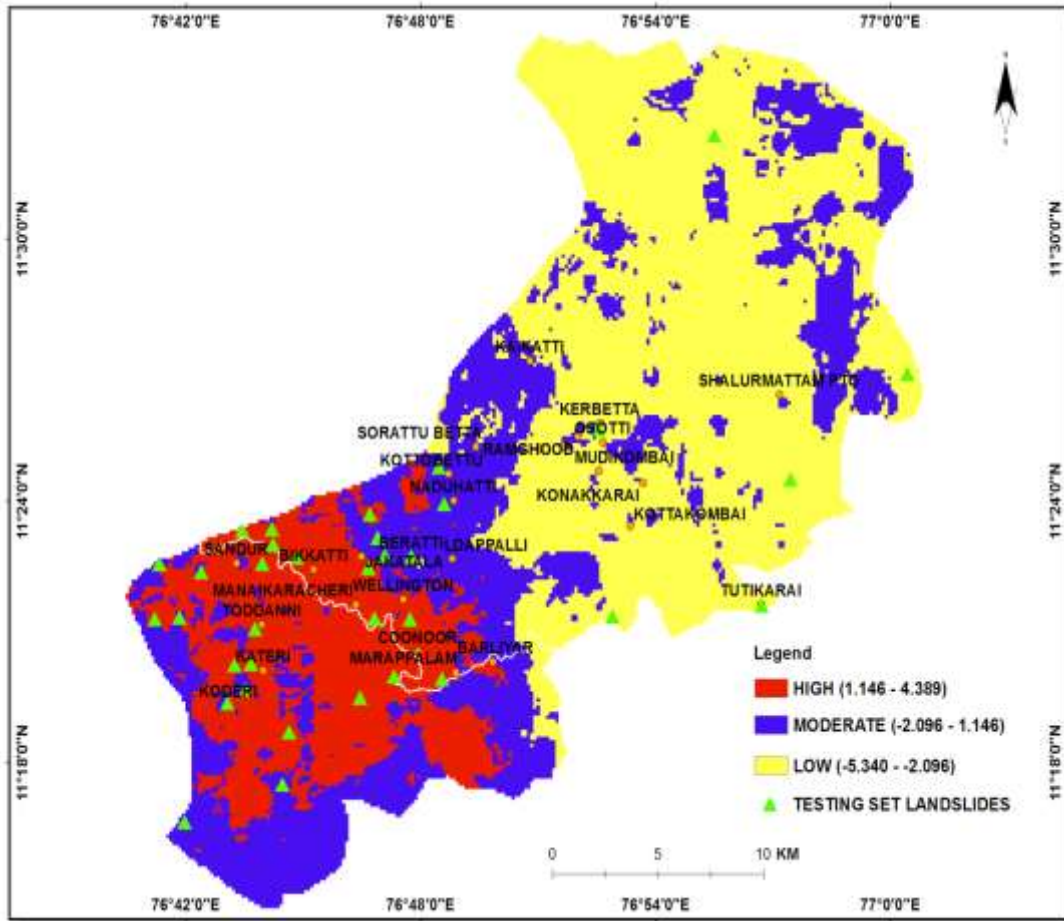


Figure 4: Landslide susceptibility map

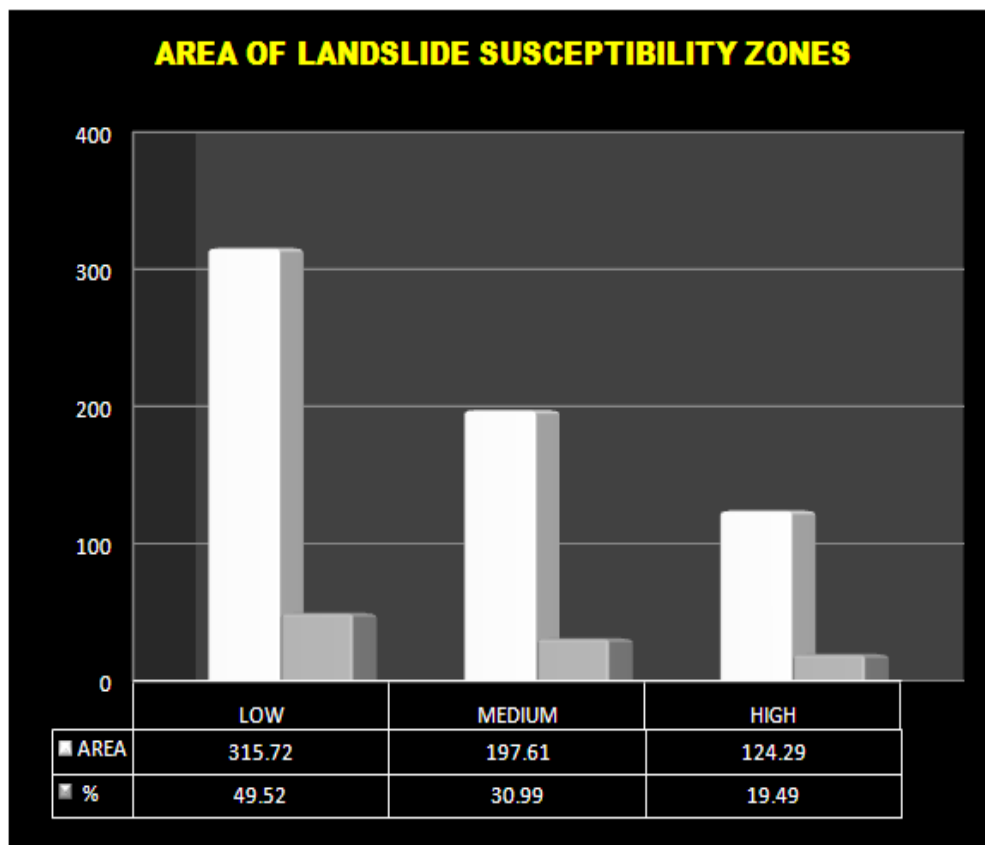


Figure 5: Graphical representation of landslide susceptibility zone

Table 2
Landslide susceptibility classes vs area percentage

| LS Class | Area | % Area |
|----------|--------|--------|
| Low | 315.72 | 49.52 |
| Moderate | 197.61 | 30.99 |
| High | 124.29 | 19.49 |

Validation of Landslide Susceptibility Map: A relative landslide density index (R) is used to verify the results quantitatively. The landslide susceptibility map was verified using test set landslide locations 35 (30 %) and to evaluate the association between landslide inventory points and the landslide vulnerability map. The aim of validation is to evaluate performance of the hazard map. The index given by Baeza and Corominas is defined as:

$$R = \frac{(n_i/N_i)}{\sum(n_i/N_i)} \times 100 \tag{5}$$

where n_i is the number of landslides in the hazard class, 'i' and N_i are the number of cells occupying the same vulnerability class.

The R-index for each susceptible class is tabulated in table 3 and the graphical representation is shown in figure 6 pointing out the landslide distribution observed in the classes, indicating the consistency of hazard classes. It has been observed that the R-index increases with the level of susceptibility. It was concluded that landslide distribution observed in these levels indicates susceptibility levels as consistent.

Conclusion

The relative effect method as a new and a capable method in the all weather conditions without necessary expert knowledge is to determine the weight of factors. The landslide susceptibility map has been produced using the relationship between each landslide influencing factor and landslide locations. The advantages of the logarithmic function are in domain determination for output data and equality for plus and minus domains of calculating RE's. The results of the land use/land cover units, mixed built-up lands show the positive values that indicate a high possibility for landslides and also show the rapid development of urbanization in the study area.

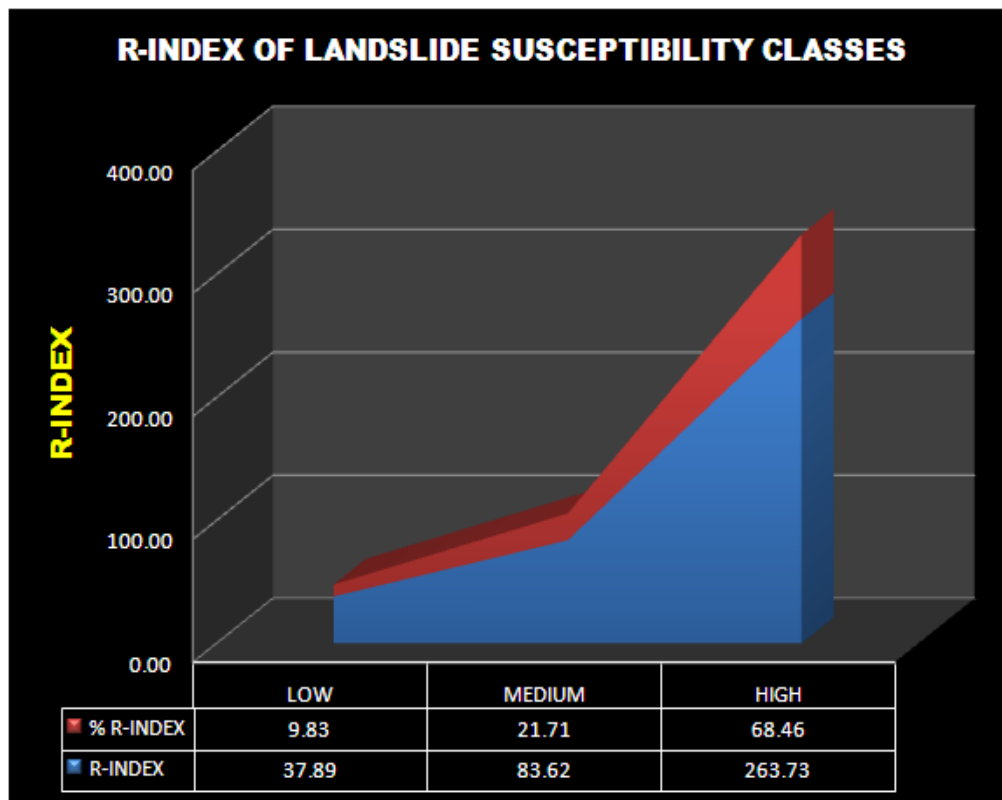


Figure 6: Graphical representation of R-index of susceptible classes

Table 3
R-index of landslide susceptibility classes

| LS Class | Pixels in Class | Class Ratio | No. of Testing Landslides in Class | Slide Ratio | R-Index |
|----------|-----------------|-------------|------------------------------------|-------------|---------|
| Low | 13335 | 45.25 | 6 | 17.14 | 3.89 |
| Moderate | 10069 | 34.17 | 10 | 28.57 | 83.62 |
| High | 6066 | 20.58 | 19 | 54.29 | 263.73 |

In geomorphic units, less dissected undulating plateau shows the positive values. In lineament density concern, very high density areas have positive values; it has been demonstrated to be the reflection of pore pressure increased during the rainy seasons leading to landslides. In the case of rainfall, 1637.23mm to 2043.51mm ranges are to very high rainfall areas having positive values wherever moderately eroded gravelly soil types are prone to landslides in the study area. Finally, all the relative effective areas of the individual parameters are integrated using GIS. Based on landslide susceptibility index, the landslide hazard map was prepared. It is observed that low prone areas are 315.72km² which is 49.52 % of the study area, moderate 197.61km² (30.99 %) and high-susceptibility zones are 124.29km² (19.49 %). The susceptibility map was validated using R-index method. The validation of the results showed that the values of 263.73 in the high susceptibility zone were indicating R-index increases with the level of susceptibility. Thus, it was considered that the RE model provides more satisfactory and reliable results. The landslide susceptibility map is the source for decision making and development activities in an area. Hence, it is concluded that the landslide susceptibility map can be used to reduce damage associated with landslides, land use planning and decision of administrative division.

Acknowledgement

The first author would like to thank the University Grants Commission, New Delhi for financial support for this part of Ph.D. work under the scheme of RGNF.

References

1. Abolghasem Akbari, Fadzil Bin Mat Yahaya, Mahmoud Azamirad and Mohsen Fanodi, Landslide susceptibility mapping using logistic regression analysis and GIS tools, *Electron J. Geotech. Eng.*, **19**, 1687-1696 (2014)
2. AGS, Guidelines for landslide susceptibility, hazard and risk zoning for land use planning, *Aust. Geomech.*, **42**, 13-36 (2007)
3. Amar Deep Regmi, Krishna Chandra Devkota, Kohki Y oshida, Biswajeet Pradhan, Hamid Reza Pourghasemi, Takashi Kumamoto and Aykut Akgun, Application of frequency ratio, statistical index and weights-of evidence models and their comparison in landslide susceptibility mapping in Central Nepal Himalaya, *Arab. J. Geosci.*, **7**(2), 725-742 (2014)
4. Ananta Man Singh Pradhan and Yun-Tae Kim, Relative effect method of landslide susceptibility zonation in weathered granite soil: a case study in Deokjeok-ri Creek, South Korea, *Nat. Hazards*, **72**(2), 1189-1217 (2014)
5. Anbalagan R., Rohan Kumar, Kalamegam Lakshmanan, Sujata Parida and Sasidharan Neethu, Landslide hazard zonation mapping using frequency ratio and fuzzy logic approach, a case study of Lachung Valley, Sikkim, *Geoenvironmental Disasters*, **2**(6), 1-17 (2015)
6. Anderson M.G. and Holcombe E., Community-based landslide risk reduction-managing disasters in small steps, The World Bank, Washington, DC (2013)
7. Baeza C. and Corominas J., Assessment of shallow landslide susceptibility by means of multivariate statistical techniques, *Earth Surf. Proc. Land*, **26**, 1251-1263 (2001)
8. Brabb E.E., Innovative approaches to landslide hazard and risk mapping, Proceedings of 4th International Symposium on Landslides, Totonto, Canada, vol. 1, BiTech Publishers, Vancouver, 307-324 (1984)
9. Devoli G., Morales A. and Hoeg K., Historical landslides in Nicaragua - collection and analysis of data, *Landslides*, **4**(1), 5-18 (2007)
10. Dilip Kumar, Neha lakhwan and Anita Rawat, Study and Prediction of Landslide in Uttarkashi, Uttarakhand, India Using GIS and ANN, *Am. J. Neural Networks and Appl.*, **3**(6), 63-74 (2017)
11. Dimitrios Myronidis, Charalambos Papageorgiou and Stavros Theophanous, Landslide susceptibility mapping based on landslide history and analytic hierarchy process (AHP), *Nat. Hazards*, **81**(1), 245 -263 (2016)
12. Ghafoori M., Sadeghi H., Lashkaripour G.R. and Alimohammadi B., Landslide hazard zonation using the relative effect method, The 10th IAEG International Congress (IAEG2006) At: Nottingham, United Kingdom, 474 (2006)
13. Gokce Deniz Hasekiogullari and Murat Ercanoglu, A new approach to use AHP in landslide susceptibility mapping: a case study at Yenice (Karabuk, NW Turkey), *Nat. Hazards*, **63**(2), 1157 -1179 (2012)
14. Gokhan Demir, Mustafa Aytekin and Aykut Akgun, Landslide susceptibility mapping by frequency ratio and logistic regression methods: an example from Niksar-Resadiye, Tokat, Turkey, *Arab. J. Geosci.*, **8**(3), 1801-1812 (2015)
15. Gokhan Demir, Mustafa Aytekin, Aykut Akgun, Sabriye Banu Ikizler and Orhan Tatar, A comparison of landslide susceptibility mapping of the eastern part of the North Anatolian Fault Zone (Turkey) by likelihood frequency ratio and analytic hierarchy process methods, *Nat. Hazards*, **65**(3), 1481-1506 (2013)
16. Jin Son, Jangwon Suh and Hyeong-Dong Park, GIS-based landslide susceptibility assessment in Seoul, South Korea, applying the radius of influence to frequency ratio analysis, *Environ. Earth Sci.*, **75**, 310 (2016)
17. Lee S., Choi J. and Woo I., The effect of spatial resolution on the accuracy of landslide susceptibility mapping: a case study in Boun, Korea, *Geosci. J.*, **8**(1), 51-60 (2004)
18. Matebie Meten, Netra Prakash Bhandary and Ryuichi Yatabe, GIS-based frequency ratio and logistic regression modelling for landslide susceptibility mapping of Debre Sina area in central Ethiopia, *J. Mt. Sci.*, **12**(6), 1355-1372 (2015)
19. Mehebut Sahana and Haroon Sajjad, Evaluating effectiveness of frequency ratio, fuzzy logic and logistic regression models in assessing landslide susceptibility: a case from Rudraprayag district, India, *J. Mt. Sci.*, **14**(11), 2150-2167 (2017)
20. Naveen Raj T., Ram Mohan V., Backiaraj S. and Muthusamy S., Landslide hazard zonation using the relative effect method in

south eastern part of Nilgiris, Tamilnadu, India, *Int. J. Eng. Sci. Technol.*, **3(4)**, 3260-3266 (2011)

21. Neelakantan R. and Yuvaraj S., Relative effect-based landslide hazard zonation mapping in parts of Nilgiris, Tamil Nadu, South India, *Arab. J. Geosci.*, **6**, 4207–4213 (2013)

22. Prabin Kayastha, Subeg Man Bijukchhen, Megh Raj Dhital and Florimond De Smedt, GIS based landslide susceptibility mapping using a fuzzy logic approach: A case study from Ghurmi-Dhad Khola area, Eastern Nepal, *J. Geol. Soc. India*, **82(3)**, 249–261 (2013)

23. Qingfeng Ding, Wei Chen and Haoyuan Hong, Application of frequency ratio, weights of evidence and evidential belief function models in landslide susceptibility mapping, *Geocarto. Int.*, **32(6)**, 619-639 (2017)

24. Ramasamy S.M., Neelakantan R. and Suresh Francis, Predictive and modeling for landslides in the Nilgiris, South India using remote sensing and GIS, In *Landslides perception and initiatives of DST*, Eds., Avasthy R.K., Bhoop Singh and Sivakumar R., Indian Soc. Eng. Geol., 177-203 (2006)

25. Soyung Park, Chuluong Choi, Byungwoo Kim and Jinsoo Kim, Landslide susceptibility mapping using frequency ratio, analytic hierarchy process, logistic regression and artificial neural network methods at the Inje area, Korea, *Environ. Earth Sci.*, **68(5)**, 1443–1464 (2013)

26. Uvaraj S. and Neelakantan R., Fuzzy logic approach for landslide hazard zonation mapping using GIS: a case study of Nilgiris, *Model Earth Syst. Environ.*, **4(2)**, 685-698 (2018)

27. Vahid Nourani, Biswajeet Pradhan, Hamid Ghaffari and Seyed Saber Sharifi, Landslide susceptibility mapping at Zonouz Plain, Iran using genetic programming and comparison with frequency ratio, logistic regression and artificial neural network models, *Nat. Hazards*, **71(1)**, 523–547 (2014)

28. Vakhshoori V. and Zare M., Landslide susceptibility mapping by comparing weight of evidence, fuzzy logic and frequency ratio methods, *Geomat. Nat. Haz. Risk*, **7(5)**, 1-41 (2016)

29. Van Westen C.J., Seijmonsbergen A.C. and Mantovani F., Comparing landslide hazard maps, *Nat. Hazards*, **20**, 137-158 (1999)

30. Wang H.B., Li J.M., Zhou B., Zhou Y., Yuan Z.Q. and Chen Y.P., Application of a hybrid model of neural networks and genetic algorithms to evaluate landslide susceptibility, *Geoenviron. Disasters*, **4**, 15 (2017)

31. Yacine Achour, Abderrahmane Boumezbeur, Riheb Hadji, Abdelmadjid Chouabbi, Victor Cavaleiro and El Amine Bendaoud, Landslide susceptibility mapping using analytic hierarchy process and information value methods along a highway road section in Constantine, Algeria, *Arab. J. Geosci.*, **10**, 194 (2017)

32. Yilmaz I., Marschalko M. and Bednarik M., Comments on Landslide susceptibility zonation study using remote sensing and GIS technology in the Ken-Betwa River Link area, India, by Avtar R., Singh C.K., Singh G., Verma R.L., Mukherjee S. and Sawada H., *Bull. Eng. Geol. Environ.*, **71**, 803–805 (2012).

(Received 25th October 2020, accepted 05th January 2021)